

## Preparation, characterization and microcalorimetric studies of nickel–iron hydrotalcites and their decompositions

Mai Tu, Jianyi Shen\*, Yi Chen

*Department of Chemistry, Nanjing University, Nanjing 210093, China*

Received 6 October 1996; accepted 22 May 1997

### Abstract

Ni–Fe hydrotalcites with Ni/Fe molar ratios of 1, 2, 3, 6 and 10 were prepared by coprecipitation. TG–DTA results showed that the hydrotalcites decomposed in two stages, corresponding to two endothermic peaks around 200 and 300°C. After calcination at 400°C, the hydrotalcites were converted to NiFeO mixed oxides with high surface areas around 100 m<sup>2</sup>/g, which exhibited the XRD pattern of NiO only. TPR studies of the mixed oxides indicated that the reduction temperatures decreased with increasing Ni content, inconsistent with the in situ Mössbauer spectroscopic results which showed that the mixed oxide (Ni/Fe = 2) was easier to reduce than the Fe<sub>2</sub>O<sub>3</sub> sample. Microcalorimetric adsorption of NH<sub>3</sub> and CO<sub>2</sub> revealed that the mixed oxide (Ni/Fe = 2) displayed intermediate acidity and basicity between those of the pure oxide NiO and Fe<sub>2</sub>O<sub>3</sub>. The mixed oxides after calcination at 800°C possessed the phases of NiO and NiFe<sub>2</sub>O<sub>4</sub> with the surface area around 15 m<sup>2</sup>/g, which exhibited moderate basicity with only a little weak acidity. © 1997 Elsevier Science B.V.

**Keywords:** Ni–Fe hydrotalcite; NiFeO mixed oxides; TG–DTA; Adsorptive microcalorimetry; Surface acidity and basicity

### 1. Introduction

Catalysts consisting of nickel and iron have frequently attracted much attention [1–10]. Supported Ni–Fe alloys have been studied in relation to the Fisher–Tropsch synthesis and methanation [1–6]. NiFeO mixed oxides have newly been found to exhibit excellent activity for the vapor phase oxidation of benzoic acid to phenol, which is one of the most important starting materials for various chemicals [7,8]. Moreover, the mixed oxides have also been investigated in catalyzing the decomposition of hydrogen peroxide [9,10].

Hydrotalcite like compounds consist of brucite-type layers containing octahedrally coordinated bivalent and trivalent cations as well as interlayer anions and water [11,12]. The anionic clays have been widely studied as precursors of catalysts and catalyst supports [11,13–21]. The mixed oxides derived from hydrotalcite-type precursors usually have high surface areas and hence may be promising materials in catalysis [11–14,20,21].

Microcalorimetry is an effective technique for investigating properties of the surface active sites of catalysts by measuring the adsorption heat evolved when a reactive molecule contacts the surface [21–28]. This heat change is related to the energy of the bonds formed between probe molecules and surface sites and hence to the nature of the bonds and the

\*Corresponding author. Fax: 008625-3317761; e-mail: physchem@netra.nju.edu.cn

chemical reactivity of the catalyst. In many cases, the calorimetric results may be correlated to catalytic activity and selectivity [22,23,28,29].

The objective of this work was to study the common properties of the Ni–Fe mixed oxides obtained from hydrotalcite-type precursors. We synthesized a series of Ni–Fe hydrotalcites with Ni/Fe molar ratios from 1 to 10 using coprecipitation method [11,20]. The resulting hydrotalcites were decomposed into NiFeO mixed oxides and were further reduced to Ni–Fe alloys. The properties of all the samples were characterized by X-ray diffraction (XRD), thermogravimetric-differential thermal analysis (TG–DTA), Mössbauer spectroscopy and temperature program reduction (TPR). In particular, ammonia and carbon dioxide were used as probe molecules to determine the surface acidity and basicity of the calcined Ni–Fe hydrotalcites.

## 2. Experimental

### 2.1. Materials

All the starting materials were AR chemicals. Ni–Fe hydrotalcites with Ni/Fe molar ratios of 1, 2, 3, 6 and 10 were prepared by coprecipitation. In each batch,  $\text{Ni}(\text{NO}_3)_2 \cdot 6\text{H}_2\text{O}$  and  $\text{Fe}(\text{NO}_3)_3 \cdot 9\text{H}_2\text{O}$  were dissolved to obtain an aqueous solution of 250 cm<sup>3</sup> with total cation concentrations of 1 M. NaOH and  $\text{Na}_2\text{CO}_3$  were dissolved to form another solution of 250 cm<sup>3</sup> with appropriate amount according to the equations of  $[\text{OH}^-] = 2[\text{Ni}^{2+}] + 2[\text{Fe}^{3+}]$  and  $[\text{CO}_3^{2-}] = 0.5[\text{Fe}^{3+}]$ . The two solutions were added dropwise to 300 cm<sup>3</sup> distilled water at 60°C over 30 min. The pH of the slurry was controlled to be in the range 8 to 9. It was aged for another 30 min at 60°C, the coprecipitate was filtered and washed until the pH of the filtered water was near to 7. The material isolated was dried at 80°C overnight. Samples with Ni/Fe molar ratio of *n* are referred to as *n*NF–HT. For comparison, pure  $\text{Ni}(\text{OH})_2$  and  $\text{Fe}(\text{OH})_3$  were also prepared in the similar manner. The hydrotalcite precursors were calcined in air for 6 h at 400 and 800°C, respectively, to produce the mixed oxides, denoted as *n*NFO–t. For example, 3NFO-400 refers to the NiFeO mixed oxide with Ni/Fe molar ratio of 3 after calcination at 400°C.

### 2.2. Apparatus

XRD patterns of the samples were measured on a Shimadzu DX-3A X-ray diffractometer equipped with a diffracted beam graphite monochromator using the  $\text{FeK}_\alpha$  radiation.

TG–DTA experiments were performed in flowing air, 60 cm<sup>3</sup> min<sup>-1</sup> on a Rigaku thermoanalyzer (Simultaneous TG–DTA High Temp. Type Cat. No. 8076E1) in the temperature range of 30–630°C and a heating rate of 20°C min<sup>-1</sup>.  $\alpha\text{-Al}_2\text{O}_3$  powder was applied as the DTA standard.

The BET surface areas of the calcined samples were measured by N<sub>2</sub> adsorption at –195.8°C using the BET method. The samples were typically evacuated to 0.7 Pa at 400°C before the measurements.

In the TPR experiments, the samples were first purged with N<sub>2</sub> at 100°C for 1 h. After cooled to room temperature, the samples were exposed to an H<sub>2</sub>/Ar mixture (H<sub>2</sub>/Ar = 0.05, molar ratio) and heated at a programming rate of 16°C min<sup>-1</sup> to a final temperature of 800°C.

Mössbauer spectra were collected at room temperature using a constant acceleration spectrometer equipped with a <sup>57</sup>Co/Pd source. The velocity scale of the spectrometer was calibrated with the <sup>57</sup>Fe Mössbauer resonance. The reduction properties were investigated by heating the samples in H<sub>2</sub> at constant temperatures followed by phase determination with in situ Mössbauer spectroscopy. The spectra were computer-fitted to Lorentzian line shapes.

Microcalorimetric measurements of adsorption of ammonia and carbon dioxide were carried out at 150°C using a Tian-Calvet heat-flow microcalorimeter [30]. The apparatus was linked to gas-handling and volumetric adsorption system, equipped with a Baratron capacitance manometer for precision pressure measurement. Heat-flow signals were detected by a transducer assembly manufactured by the ITI Inc. The differential heat of adsorption versus adsorbate coverage was determined by measuring the heats evolved when doses of gas (1–3 μmol) were introduced sequentially onto the sample until a final equilibrium pressure was reached at 700 Pa. Before a measurement, the sample was calcined in high purity oxygen at 400°C for 2 h and evacuated at 400°C for another 2 h. Ammonia and carbon dioxide (purity > 99.995%)

were purified by successive freeze-pump-thaw cycles before used.

### 3. Results and discussion

As can be seen from the XRD patterns, shown in Fig. 1, a typical hydroxalcite type structure was present in all the samples with Ni/Fe ratio from 1 to 10 [11]. The hydroxalcites have a rhombohedral R-3m symmetry, in which the  $\text{Ni}^{2+}$  and  $\text{Fe}^{3+}$  cations are incorporated into brucite-type layers and the excessive positive charges on the layers are compensated by carbonate anions in the interlayers [11]. The intensity of the diffraction peaks are weak, which may be in part be attributed to the poor crystallinity of all the Ni–Fe hydroxalcites. However, no other separated phases were detected in these samples.

TG–DTA profiles of some Ni–Fe hydroxalcites as well as  $\text{Fe}(\text{OH})_3$  and  $\text{Ni}(\text{OH})_2$  are reported in Fig. 2. These hydroxalcites exhibit two similar weight loss stages. The first endothermic peak at about  $200^\circ\text{C}$  corresponds to the loss of interlayer water without collapse of the hydroxalcite structure. The second endothermic peak at about  $300^\circ\text{C}$  was due to the loss of hydroxyl groups from the brucite-like layer and the interlayer  $\text{CO}_3^{2-}$  anions. In addition, a little water was obviously adsorbed on the surfaces of the hydroxalcites and it desorbed below  $100^\circ\text{C}$ .  $\text{Ni}(\text{OH})_2$  and  $\text{Fe}(\text{OH})_3$  exhibit totally different decomposition behavior.

The formula of Ni–Fe hydroxalcite can be calculated from the TG results, for example, sample 3NF-HT composed of  $\text{Ni}_6\text{Fe}_2(\text{OH})_{16}\text{CO}_3 \cdot (X_1 + X_2)\text{H}_2\text{O}$ , in

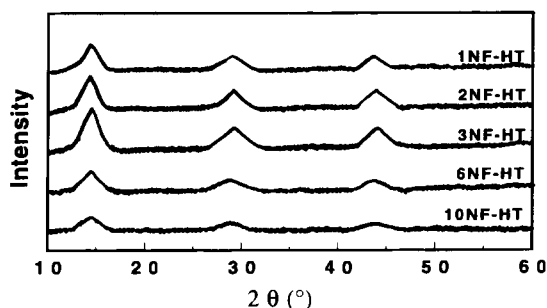


Fig. 1. XRD patterns of the Ni–Fe hydroxalcites with Ni/Fe molar ratios of 1, 2, 3, 6 and 10.

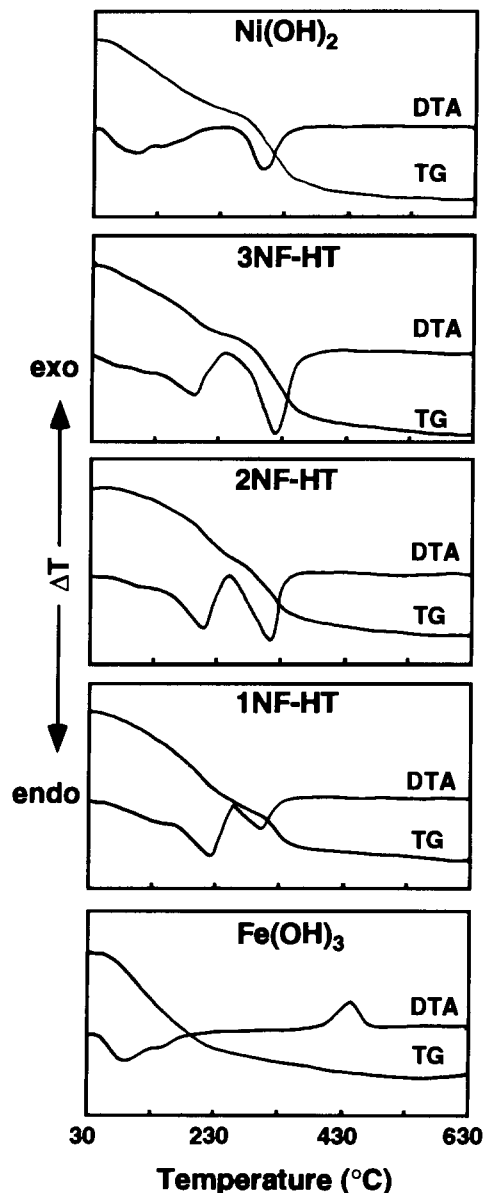


Fig. 2. TG–DTA profiles of the Ni–Fe hydroxalcites,  $\text{Ni}(\text{OH})_2$  and  $\text{Fe}(\text{OH})_3$ .

which  $X_1$  and  $X_2$  denote the number of surface and interlayer water molecules, respectively. The formula of 3NF-HT is  $\text{Ni}_6\text{Fe}_2(\text{OH})_{16}\text{CO}_3 \cdot 4.0\text{H}_2\text{O}$ , in agreement with that of the natural one, Reevesite [31].

The XRD patterns of the calcined Ni–Fe hydroxalcites are shown in Fig. 3. Only three broad peaks

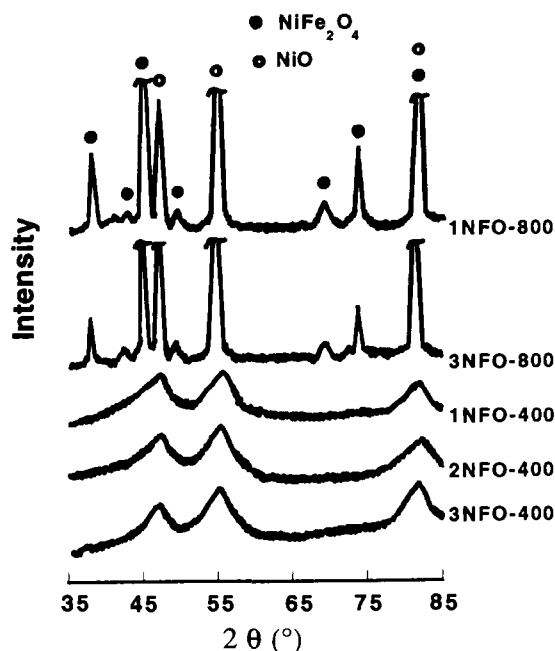


Fig. 3. XRD patterns of the calcined Ni-Fe hydrotalcites.

with  $d$  values around 2.09, 2.41 and 1.48 (characteristic of NiO) can be observed for all the samples calcined at 400°C. The absence of any detectable iron phase suggests that the  $\text{Fe}^{3+}$  cations are highly dispersed in the NiO lattice. After calcination at 800°C, the mixed oxides showed sharp diffraction peaks due to NiO and  $\text{NiFe}_2\text{O}_4$  spinel phase, respectively. The intensity of the diffraction lines of  $\text{NiFe}_2\text{O}_4$  increased as the increase of Fe content.

Table 1 gives the BET surface areas of some calcined Ni-Fe hydrotalcites. The samples calcined at 400°C had similar surface areas (around  $100 \text{ m}^2 \text{ g}^{-1}$ ). All the mixed oxides obtained from hydrotalcite-type precursors [11,20,21] have high surface areas. It was interesting that the samples had surface areas around  $15 \text{ m}^2 \text{ g}^{-1}$  even after calcination at 800°C. Miki et al.

Table 1  
BET surface areas of the NiFeO mixed oxides after calcination at 400 and 800°C

Sample	1NFO-400	2NFO-400	3NFO-400	6NFO-400	10NFO-400
BET areas ( $\text{m}^2/\text{g}$ )	107	102	121	93	117
Sample	$\text{Fe}_2\text{O}_3$ -400	NiO-400	1NFO-800	2NFO-800	3NFO-800
BET areas ( $\text{m}^2/\text{g}$ )	46	50	18	15	13

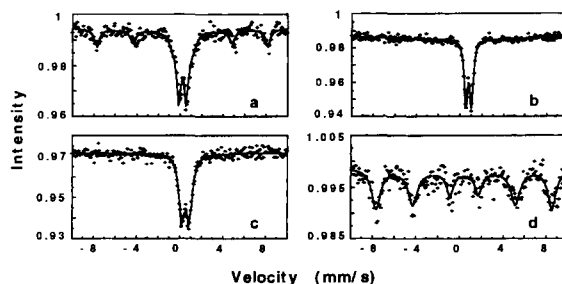


Fig. 4. Mössbauer spectra of the  $\text{Fe}_2\text{O}_3$  sample (a) as well as the Ni-Fe hydrotalcites (Ni/Fe = 2) before (b) and after calcination at 400 (c) and 800°C (d).

prepared the NiFeO mixed oxides with ordinary coprecipitation without formation of hydrotalcite structure [7,8]. They pointed out that the active species for the vapor phase oxidation of benzoic acid to phenol might be the finely dispersed NiO in  $\text{NiFe}_2\text{O}_4$  and the larger surface areas of the catalysts would result in higher activities for the reaction. In our case, we obtained the exact phases in the samples calcined at 800°C as detected by XRD and Mössbauer. This suggests that the method presented here may be a way for the preparation of NiFeO catalysts for the oxidation of benzoic acid to phenol.

Fig. 4 presents the Mössbauer spectra for the Ni-Fe hydrotalcites before and after calcination in comparison with those of pure iron oxide samples. The Mössbauer parameters are summarized in Table 2. The hydrotalcite and the one calcined at 400°C displayed a doublet due to the superparamagnetic  $\text{Fe}^{3+}$  species with isomer shifts of  $0.77 \text{ mm s}^{-1}$  and  $0.52 \text{ mm s}^{-1}$ , respectively (Fig. 4(b,c)). The absence of a magnetically split six-finger pattern, as was found in Fig. 4(a) for the iron oxide calcined at 400°C, indicates that the particles of iron species in the 2NFO-400 sample might be smaller than 10 nm [32]. This result is consistent with the previous XRD results that  $\text{Fe}^{3+}$  cations were highly dispersed

Table 2

Mössbauer parameters of the Ni–Fe hydrotalcites and NiFeO mixed oxides treated at different conditions

Sample	Treatment	IS (mm/s)	QS (mm/s)	HF (kOe)	Assignment
2NF-HT	140°C dried	0.77	0.53		Fe <sup>3+</sup>
2NFO-400	400°C calcined	0.52	0.69		Fe <sup>3+</sup>
	800°C calcined	0.52		501	NiFe spinel
	300°C reduced	0.49		297	NiFe alloy
	400°C reduced	0.46		296	NiFe alloy
Fe <sub>2</sub> O <sub>3</sub> -400	400°C calcined	0.37		510	α-Fe <sub>2</sub> O <sub>3</sub>
	300°C reduced	0.25	0.02	488	Fe <sub>3</sub> O <sub>4</sub> (Td)
		0.62	0.09	456	Fe <sub>3</sub> O <sub>4</sub> (Oh)
	400°C reduced	-0.03	0	329	α-Fe

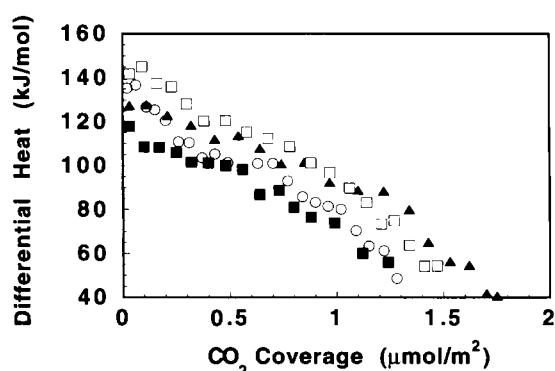


Fig. 5. Differential heat versus CO<sub>2</sub> coverage at 150°C on the Ni–Fe hydrotalcites (Ni/Fe = 2) calcined at 400 (○) and 800°C (▲) as well as the Fe<sub>2</sub>O<sub>3</sub> (■) and NiO (□) calcined at 400°C.

in the NiO lattice of the calcined hydrotalcites. As can be seen in Fig. 4(d), the hydrotalcite calcined at 800°C displays a sextuplet (IS = 0.52 mm s<sup>-1</sup>) with a magnetic hyperfine field of 501 kOe, corresponding to the NiFe<sub>2</sub>O<sub>4</sub> spinel phase [33].

In Fig. 5 the results of the microcalorimetric adsorption of CO<sub>2</sub> on to samples of calcined Ni–Fe hydrotalcite (Ni/Fe = 2), NiO and Fe<sub>2</sub>O<sub>3</sub> are shown. It is seen that NiO displayed the strongest basicity with an initial heat of 145 kJ mol<sup>-1</sup> and the saturation coverage of 1.5 μmol m<sup>-2</sup> for the CO<sub>2</sub> adsorption. Fe<sub>2</sub>O<sub>3</sub> exhibited the weakest basicity from the point of view of both the initial heat (120 kJ mol<sup>-1</sup>) and saturation coverage (1.2 μmol m<sup>-2</sup>). In contrast, the Ni–Fe mixed oxide calcined at 400°C possess intermediate basicity: the initial adsorption heat was about 135 kJ mol<sup>-1</sup> and the saturation coverage was about

1.3 μmol m<sup>-2</sup>. The Sanderson electronegativity scale can be used to explain the acidity and basicity of oxide catalysts [22,23,34]. To a first approximation, the oxide with lower Sanderson electronegativity is a stronger base and weaker acid. Here, we correlate the strength of the basicity characteristic of the initial heat of CO<sub>2</sub> adsorption to the Sanderson electronegativity. The Sanderson electronegativity of the sample increased following the order: NiO(2.26) < the mixed oxide with Ni/Fe = 2 (2.33) < Fe<sub>2</sub>O<sub>3</sub> (2.46), in agreement with the calorimetric results that the calcined Ni–Fe hydrotalcite possessed an intermediate basicity. Shown in parentheses are the Sanderson electronegativities of these oxides [35]. It is interesting that the hydrotalcite calcined at 800°C exhibited a similar initial heat for CO<sub>2</sub> adsorption to that of the sample calcined at 400°C. However, the 800°C calcined sample exhibited denser basic sites than the one calcined at 400°C.

Fig. 6 shows the results of microcalorimetric adsorption of NH<sub>3</sub> on the samples. It is surprising that the NiO displays a very high initial heat (~250 kJ mol<sup>-1</sup>). This may be due to the coordination reaction between NH<sub>3</sub> and nickel cations instead of simple chemisorption of NH<sub>3</sub> on the surface. The initial heat and coverage for the adsorption of NH<sub>3</sub> on Fe<sub>2</sub>O<sub>3</sub> are 110 kJ/mol<sup>-1</sup> and 3.5 μmol/m<sup>-2</sup>, respectively. The 400°C calcined hydrotalcite displayed similar initial heat (~120 kJ/mol<sup>-1</sup>) and smaller coverage (~2.4 μmol/m<sup>-2</sup>) than the Fe<sub>2</sub>O<sub>3</sub>. Apparently, the behavior of NH<sub>3</sub> adsorption on the 400°C calcined hydrotalcite was closer to Fe<sub>2</sub>O<sub>3</sub>, indicating that the adsorption of NH<sub>3</sub> on the mixed oxide sample was mainly related to iron cations

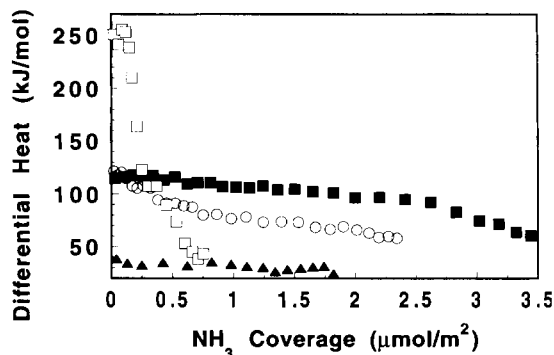


Fig. 6. Differential heat versus  $\text{NH}_3$  coverage at  $150^\circ\text{C}$  on the Ni-Fe hydrotalcites (Ni/Fe = 2) calcined at  $400^\circ\text{C}$  (○) and  $800^\circ\text{C}$  (▲) as well as the  $\text{Fe}_2\text{O}_3$  (■) and NiO (□) calcined at  $400^\circ\text{C}$ .

instead of nickel cations. The  $800^\circ\text{C}$  calcined hydrotalcite exhibited totally different behavior for the  $\text{NH}_3$  adsorption. The change in heat versus coverage plot displays a plateau for this sample with the heat of adsorption around  $40\text{ kJ mol}^{-1}$ . It is generally accepted that the strength of Lewis acidity is related to the degree of unsaturation of a cation that adsorbs an  $\text{NH}_3$  molecule, that is, a higher unsaturated site exhibits stronger Lewis acidity. In the light of this, we concluded that the unsaturation of cations on the surface of the  $800^\circ\text{C}$  calcined mixed oxide was greatly diminished, leading to weak acidity for the sample. Comparing the results for the adsorption of  $\text{CO}_2$  and  $\text{NH}_3$ , we suggest that the Ni-Fe mixed oxide calcined at  $800^\circ\text{C}$  was moderate solid base with weak acidity.

TPR and in situ Mössbauer spectroscopy were employed to investigate the reducibility of the calcined Ni-Fe hydrotalcite samples. Fig. 7 presents the TPR profiles of the samples after calcination at  $400^\circ\text{C}$ . A reduction peak around  $550^\circ\text{C}$ , with a low temperature shoulder around  $450^\circ\text{C}$ , was observed for all the samples except for the 10NFO-400. The reduction temperature decreased slightly with increase in the Ni/Fe molar ratios from 1 to 6, while the 10NFO-400 was much easier to reduce than the others. This is consistent with the Mössbauer result which will be discussed shortly.

The Mössbauer spectra of the samples after reduction in  $\text{H}_2$  are shown in Fig. 8 and the Mössbauer parameters are listed in Table 2. Upon reduction at  $300^\circ\text{C}$ , the NiFeO mixed oxide (Ni/Fe = 2) displayed

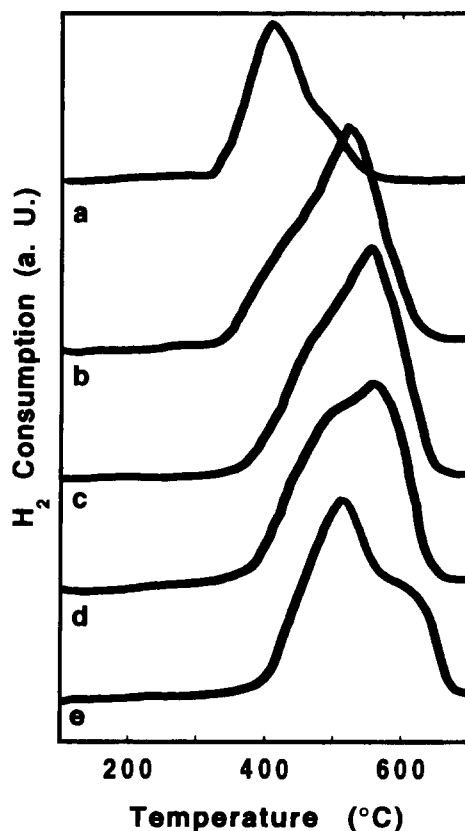


Fig. 7. TPR profiles of the Ni-Fe hydrotalcites with Ni/Fe molar ratios of 10 (a), 6 (b), 3 (c), 2 (d), and 1 (e) calcined at  $400^\circ\text{C}$ .

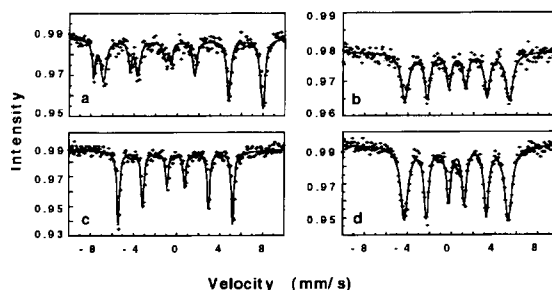


Fig. 8. Mössbauer spectra of the  $\text{Fe}_2\text{O}_3$  reduced at  $300^\circ\text{C}$  (a) and  $400^\circ\text{C}$  (c) as well as the NiFeO mixed oxides (Ni/Fe = 2) reduced at  $300^\circ\text{C}$  (b) and  $400^\circ\text{C}$  (d).

a sextet with a hyperfine field of 297 kOe (Fig. 8(b)), attributed to Ni-Fe alloy [6,36]. In contrast, the  $\text{Fe}_2\text{O}_3$  was reduced to magnetite at  $300^\circ\text{C}$  (Fig. 8(a)). The reduction of  $\text{Fe}_2\text{O}_3$  at  $400^\circ\text{C}$  resulted in the formation

of  $\alpha$ -Fe (329 kOe) as shown in Fig. 8(c). Apparently, the existence of nickel greatly enhanced the reducibility of the iron species, in agreement with the results reported by Unmuth et. al. for the supported Ni–Fe catalysts [2].

#### 4. Conclusions

The main conclusions obtained are as follows:

1. Ni–Fe hydrotalcites with Ni/Fe molar ratios of 1, 2, 3, 6 and 10 can be prepared by a coprecipitation method. The hydrotalcites decomposed in two stages at about 200 and 300°C, respectively, corresponding to the successive loss of interlayer water, carbonate and hydroxyl groups. Thus, calcination at 400°C is enough to obtain Ni–Fe mixed oxides from their hydrotalcite precursors. In addition, the formula of the hydrotalcite with the Ni/Fe ratio of 3 was found to be  $\text{Ni}_6\text{Fe}_2(\text{OH})_{16}\text{CO}_3 \cdot 4.0\text{H}_2\text{O}$  using the results of TG–DTA. The composition was similar to that of Reevesite as found in nature.
2. The Ni–Fe hydrotalcites calcined at 400°C exhibited high surface areas around  $100 \text{ m}^2 \text{ g}^{-1}$  and displayed XRD patterns of NiO only indicating that the  $\text{Fe}^{3+}$  cations were highly dispersed in the lattice of NiO. This was also confirmed by the Mössbauer spectrum of the sample which showed only a quadruple doublet. The mixed oxide (Ni/Fe = 2) displayed intermediate acidity and basicity compared to the pure oxide NiO and  $\text{Fe}_2\text{O}_3$  revealed by the microcalorimetric adsorption of  $\text{NH}_3$  and  $\text{CO}_2$ .
3. The 800°C calcined Ni–Fe hydrotalcite (Ni/Fe = 2) exhibited structures of NiO and  $\text{NiFe}_2\text{O}_4$  and possessed surface areas around  $15 \text{ m}^2 \text{ g}^{-1}$ . The microcalorimetric results showed that the sample was a moderated base with a little weak acidity.

#### Acknowledgements

We acknowledge the financial supports from the Trans-Century Training Program Foundation for Talents by the State Education Commission of China

and the National Natural Science Foundation of China.

#### References

- [1] G.P. Raupp and W.N. Delgass, *J. Catal.*, 58 (1979) 337.
- [2] E.E. Unmuth, L.H. Schwartz and J.B. Butt, *J. Catal.*, 61 (1980) 242.
- [3] J.A. Amelse, L.H. Schwartz and J.B. Butt, *J. Catal.*, 72 (1981) 95.
- [4] H. Arai, K. Mitsuishi and T. Seiyama, *Chem. Lett.*, (1984) 1291.
- [5] X.Z. Jiang, S.A. Stevenson and J.A. Dumesic, *J. Catal.*, 91 (1985) 11.
- [6] C.N.R. Rao, G.U. Kulkarni, K.R. Kannan and S. Chaturvedi, *J. Phys. Chem.*, 96 (1992) 7379.
- [7] J. Miki, M. Asanuma, Y. Tachibana and T. Shikada, *Appl. Catal.*, A 132 (1994) L1.
- [8] J. Miki, M. Asanuma, Y. Tachibana and T. Shikada, *J. Catal.*, 151 (1995) 323.
- [9] A.I. Onuchukwu, *J. Chem. Soc. Faraday Trans. 1*, 80 (1984) 1447.
- [10] S.K. Mazumdar and A.S. Brar, *Thermochimica Acta*, 93 (1985) 505.
- [11] F. Cavani, F. Trifiro and F. Vaccari, *Catal. Today*, 11 (1991) 173.
- [12] W.T. Reichle, *Chemtech*, January (1986) 58.
- [13] O. Clause, B. Rebours, E. Merlen, F. Trifiro and A. Vaccari, *J. Catal.*, 133 (1992) 231.
- [14] A.L. McKenzie, C.T. Fishel and R.J. Davis, *J. Catal.*, 138 (1992) 547.
- [15] R.J. Davis and E.G. Derouane, *J. Catal.*, 132 (1991) 269.
- [16] A. Corma, V. Fornes, R.M. Martin-Aranda and F. Rey, *J. Catal.*, 134 (1992) 58.
- [17] K. Fuda, N. Kudo, S. Kawai and T. Matsunaga, *Chem. Lett.*, (1993) 777.
- [18] J.M. Lopez, A. Dejoz and M.I. Vazquez, *Appl. Catal.*, A., 132 (1995) 41.
- [19] A. Corma and R.M. Martin-Aranda, *Appl. Catal.*, A 105 (1995) 271.
- [20] J. Shen, G. Bin, M. Tu and Yi Chen, *Catal. Today*, 30 (1996) 77.
- [21] J. Shen, J.M. Kobe, Yi Chen and J.A. Dumesic, *Langmuir*, 10 (1994) 3902.
- [22] N. Cardona-Martinez and J.A. Dumesic, *Adv. Catal.*, 38 (1992) 149.
- [23] A. Auroux and A. Gervasini, *J. Phys. Chem.*, 94 (1990) 6371.
- [24] R.R. Gatte and J. Phillips, *J. Catal.*, 116 (1989) 49.
- [25] J. Shen, R.D. Cortright, Yi Chen and J.A. Dumesic, *J. Phys. Chem.*, 98 (1994) 8067.
- [26] J. Shen, M.J. Lochhead, K.L. Bray, Yi Chen and J.A. Dumesic, *J. Phys. Chem.*, 99 (1995) 2384.
- [27] N. Cardona-Martinez and J.A. Dumesic, *J. Catal.*, 125 (1990) 427.
- [28] A. Gervasini, G. Bellussi, J. Fenyvesi and A. Auroux, *J. Phys. Chem.*, 99 (1995) 5117.

- [29] A. Gervasini and A. Auroux, *J. Catal.*, 131 (1991) 190.
- [30] B.E. Handy, S.B. Sharma, B.E. Spiewak and J.A. Dumesic, *Meas. Sci. Technol.*, 4 (1993) 1350.
- [31] S.A. De Waal and E.A. Viljoen, *Amer. Min.*, 62 (1977) 458.
- [32] W. Kundig, H. Bommel, G. Constabaris and R.H. Lindquist, *Phys. Rev.*, B142 (1996) 327.
- [33] T. Pannaparayil, R. Marande, S. Komarneni and S.G. Sankar, *J. Appl. Phys.*, 64 (1988) 5641.
- [34] R.T. Sanderson, *J. Am. Chem. Soc.*, 105 (1983) 2259.
- [35] J.E. Huheey, *Inorganic Chemistry: Principles of Structure and Reactivity*, 3rd ed., Harper and Row, New York, 1983, p. 936.
- [36] R.Z. Ma et al., (Ed.), *Handbook of Mössbauer spectroscopy*, 1993 p. 351.